
Automatic Discovery of Privacy–Utility Pareto Fronts

Brendan Avent*
Department of Computer Science
University of Southern California
Los Angeles, California, 90007
baavent@gmail.com

**Javier Gonzalez, Tom Diethe,
Andrei Paleyes, Borja Balle**
Amazon
Cambridge, UK
{gojav, tdiethe, paleyes, pigem}@amazon.com

Abstract

Differential privacy is a mathematical framework for privacy-preserving data analysis. Changing the hyperparameters of a differentially private algorithm allows one to trade off privacy and utility in a principled way. Quantifying this trade-off in advance is essential to decision-makers tasked with deciding how much privacy can be provided in a particular application while keeping acceptable utility. For more complex tasks, such as training neural networks under differential privacy, the utility achieved by a given algorithm can only be measured empirically. This paper presents a Bayesian optimization methodology for efficiently characterizing the privacy–utility trade-off of any differentially private algorithm using only empirical measurements of its utility. The versatility of our method is illustrated on a number of machine learning tasks involving multiple models, optimizers, and datasets.

1 Introduction

Differential privacy (DP) [14] is the de-facto standard for privacy-preserving data analysis, including the training of machine learning models using sensitive data. The strength of DP comes from its use of randomness to hide the contribution of any individual’s data from an adversary with access to *arbitrary side knowledge*. The price of DP is a loss in utility caused by the need to inject noise into computations. Quantifying the trade-off between privacy and utility is a central topic in the literature on differential privacy. Formal analysis of such trade-offs lead to algorithms achieving a pre-specified level privacy with minimal utility reduction, or, conversely, an a-priori acceptable level of utility with maximal privacy. Since the privacy level is generally regarded as a policy decision [38], this step is essential to decision-makers tasked with balancing utility and privacy in real-world deployments [3].

However, analytical analyses of the privacy–utility trade-off are only available for relatively simple problems amenable to mathematical treatment, and cannot be conducted for most problems of practical interest. Further, differentially private algorithms have more hyperparameters than their non-private counterparts, most of which affect both privacy and utility. In this paper we develop a Bayesian optimization approach for *empirically* characterizing the privacy–utility trade-off, and provide a principled, computationally efficient way to tune any differentially private algorithm.

A canonical application of our methods is differentially private deep learning. Differentially private stochastic optimization has been employed to train feed-forward [1], convolutional [8], and recurrent [35] neural networks, showing that reasonable accuracies can be achieved when selecting hyperparameters carefully. These works rely on the *gradient perturbation* technique, which clips and adds noise to gradient computations, while keeping track of the privacy loss incurred. However, these results do not provide actionable information regarding the privacy–utility trade-off of the proposed models. For example, private stochastic optimization methods can obtain the same level of privacy in different ways (e.g. by increasing the noise variance and reducing the clipping norm, or *vice-versa*),

*Corresponding author.

and it is not generally clear what combinations of these changes yield the best possible utility for a fixed privacy level. Furthermore, increasing the number of hyperparameters makes exhaustive hyperparameter optimization prohibitively expensive.

The goal of this paper is to provide a computationally efficient methodology to this problem by using Bayesian optimization to estimate the privacy–utility *Pareto front* of a given algorithm. The Pareto fronts obtained by our method can be used to find hyperparameter settings leading to the optimal operating points of any differentially private technique, enabling decision-makers to take informed actions when balancing the privacy–utility trade-off of an algorithm before deployment. This is in line with the approach taken by the U.S. Census Bureau to calibrate the level of DP that will be used when releasing the results of the upcoming 2020 census [18, 3, 2].

Our contributions are: (1) Characterizing the privacy–utility trade-off of an algorithm as a function of its hyperparameters as the problem of learning a Pareto front on the privacy vs. utility plane (Sec. 2). (2) Designing DPARETO, a multi-objective Bayesian optimization algorithm for learning the privacy–utility Pareto front of any differentially private algorithm (Sec. 3). (3) Instantiating and experimentally evaluating our framework for the case of differentially private stochastic optimization on a variety of learning tasks involving multiple models, optimizers, and datasets (Sec. 4).

2 The Privacy–Utility Pareto Front

This section provides an abstract formulation of the problem we want to address. We start by introducing some basic notation and recalling the definition of differential privacy, after which we will define the key components of our framework. We then formalize the task of quantifying the privacy–utility trade-off using the notion of Pareto front, and conclude by giving an illustrative example in the context private logistic regression trained with SGD [45].

General Setup Let $A : \mathcal{Z}^n \rightarrow \mathcal{W}$ be a *randomized algorithm* that takes as input a tuple containing n records from \mathcal{Z} and outputs a value in some set \mathcal{W} . Differential privacy formalizes the idea that A preserves the privacy of its inputs when the output distribution is stable under changes in one input.

Definition 1 (Dwork et al. [14], Dwork [13]). *Given $\varepsilon \geq 0$ and $\delta \in [0, 1]$, we say algorithm A is (ε, δ) -DP if for any pair of inputs z, z' differing in a single coordinate we have²*

$$\sup_{E \subseteq \mathcal{W}} (\mathbb{P}[A(z) \in E] - e^\varepsilon \mathbb{P}[A(z') \in E]) \leq \delta .$$

To analyze the trade-off between utility and privacy for a given problem, we consider a *parametrized* family of algorithms $\mathcal{A} = \{A_\lambda : \mathcal{Z}^n \rightarrow \mathcal{W}\}$. Here, $\lambda \in \Lambda$ indexes the possible choices of hyperparameters, so \mathcal{A} can be interpreted as the set of all possible algorithm configurations for solving a given task. For example, in the context of a machine learning application, the family \mathcal{A} consists of a set of learning algorithms which take as input a training dataset $z = (z_1, \dots, z_n)$ containing n example-label pairs $z_i = (x_i, y_i) \in \mathcal{Z} = \mathcal{X} \times \mathcal{Y}$ and produce as output the parameters $w \in \mathcal{W} \subseteq \mathbb{R}^d$ of a predictive model. It is clear that in this context different choices for the hyperparameters might yield different utilities. We further assume each configuration A_λ of the algorithm satisfies DP with potentially distinct privacy parameters.

To capture the privacy–utility trade-off across \mathcal{A} we introduce two oracles to model the effect of hyperparameter changes on the privacy and utility of A_λ . A *privacy oracle* is a function $P_\delta : \Lambda \rightarrow [0, +\infty]$ that given a choice of hyperparameters λ returns a value $\varepsilon = P_\delta(\lambda)$ such that A_λ satisfies (ε, δ) -DP. An instance-specific *utility oracle* is a function $U_z : \Lambda \rightarrow [0, 1]$ that given a choice of hyperparameters λ returns some measure of the utility³ of the output distribution of $A_\lambda(z)$. These oracles allow us to condense everything about our problem in the tuple (Λ, P_δ, U_z) . Given these three objects, our goal is to find hyperparameter settings for A_λ that simultaneously achieve maximal privacy and utility on a given input z . Next we will formalize this goal using the concept of Pareto front, but we first provide remarks about the definition of our oracles.

Remark 1 (Privacy Oracle). The choice to parametrize our privacy oracle P_δ in terms of a fixed δ stems from the convention that ε is considered the most important privacy parameter, whereas δ can

²Smaller values of ε and δ yield more private algorithms.

³Due to the broad applicability of DP, concrete utility measures are generally defined on a per-problem basis. Here we use the conventions that U_z is bounded and that larger utility is better.

be interpreted as a small probability that an $(\epsilon, 0)$ -DP guarantee fails. This choice is also aligned with recent uses of DP in machine learning where the privacy analysis is conducted under the framework of Rényi DP [36] and the reported privacy is obtained by *a posteriori* converting the guarantees to standard (ϵ, δ) -DP for some fixed δ [1, 20, 35, 17, 44]. In particular, in our experiments with gradient perturbation for SGD and other stochastic optimization methods (Sec. 4) we implement the privacy oracle using the moments accountant technique proposed [1] coupled with the tight bounds provided in [44] for Rényi DP amplification by subsampling without replacement.

Remark 2 (Utility Oracle). Parametrizing the utility oracle U_z by a fixed input is a choice justified by the type applications we tackle in our experiments (cf. Sec. 4). Other applications might require variations which our framework can easily accommodate by extending the definition of the utility oracle. We also stress that since the algorithms in \mathcal{A} are randomized, the utility $U_z(\lambda)$ is a property of the output *distribution* of $A_\lambda(z)$. This means that in practice we might have to implement the oracle approximately, e.g. through sampling. In particular, in our experiments we use a test set of measure the utility of a hyperparameter setting by running $A_\lambda(z)$ a fixed number of times R to obtain model parameters w_1, \dots, w_R , and then let $U_z(\lambda)$ be the average accuracy of the models on the test set.

The Pareto front of a collection of points $\Gamma \subset \mathbb{R}^p$ contains all the points in Γ where none of the coordinates can be decreased further without increasing some of the other coordinates (while remaining inside Γ).

Definition 2 (Pareto Front). *Let $\Gamma \subset \mathbb{R}^p$ and $u, v \in \Gamma$. We say that u dominates v if $u_i \leq v_i$ for all $i \in [p]$, and we write $u \preceq v$. The Pareto front of Γ is the set of all non-dominated points $\mathcal{PF}(\Gamma) = \{u \in \Gamma \mid v \not\preceq u, \forall v \in \Gamma \setminus \{u\}\}$.*

According to this definition, given a privacy–utility trade-off problem of the form (Λ, P_δ, U_z) we are interested in finding the Pareto front $\mathcal{PF}(\Gamma)$ of the 2-dimensional set⁴ $\Gamma = \{(P_\delta(\lambda), 1 - U_z(\lambda)) \mid \lambda \in \Lambda\}$. Given this Pareto front, a decision-maker looking to deploy DP has all the necessary information to make an informed decision about how to trade-off privacy and utility in their particular application.

Example: Logistic Regression To illustrate the ingredients of our framework we consider a simple private logistic regression model with ℓ_2 regularization trained on the Adult dataset [26]. In particular, to reduce the number of hyperparameters we privatize the model by training with mini-batched projected SGD and applying a Gaussian perturbation at the output using the method from [45, Algorithm 2] with default parameters⁵. The only hyperparameters we tune in this experiment are the regularization λ and the noise standard deviation σ , while we fix the rest of hyperparameters⁶. Note that both hyperparameters affect privacy and accuracy in this case. To implement the privacy oracle we compute the global sensitivity according to [45, Algorithm 2] and find the ϵ for a fixed $\delta = 10^{-6}$ using the exact analysis of the Gaussian mechanism provided in [6]. To implement the utility oracle we evaluate the accuracy of the model on the test set, averaging over 50 runs for each setting of the hyperparameters. Given the small number of hyperparameters, we can perform a fine grid search over $\lambda \in [10^{-4}, 1]$ and $\sigma \in [0.1, 10]$ to obtain the exact Pareto front for this problem. The results are displayed in Figure 1, where we illustrate privacy and utility as a function of both hyperparameters, as well as the resulting Pareto front and the corresponding hyperparameter settings.

Threat Model In the idealized setting presented above, the desired output is the Pareto front $\mathcal{PF}(\Gamma)$, which depends on z through the utility oracle; this is also the case for the Bayesian optimization algorithm for approximating the Pareto front presented in Sec. 3. This warrants a discussion about what threat model is appropriate to consider here.

DP guarantees that an adversary observing the output $w = A_\lambda(z)$ will not be able to infer too much about any individual record in z . The (central) threat model for DP assumes that z is owned by a trusted curator, responsible for running the algorithm and releasing its output to the world. However, the framework described above does not attempt to prevent information about z to be exposed by the Pareto front. This is because our methodology is only meant to provide a substitute for using closed-form utility guarantees when selecting hyperparameters for a given DP algorithm *before its deployment*. Accordingly, throughout this work we assume the Pareto fronts obtained with our method are only revealed to a small set of trusted individuals, which is the usual scenario in an industrial context.

⁴The use of $1 - U_z(\lambda)$ for the utility coordinate is for notational consistency, since we use the convention that the points in the Pareto front are those that minimize each individual dimension.

⁵These are the smoothness, Lipschitz and strong convexity parameters of the loss, and the learning rate.

⁶Mini-batch size $m = 1$ and number of epochs $T = 10$.

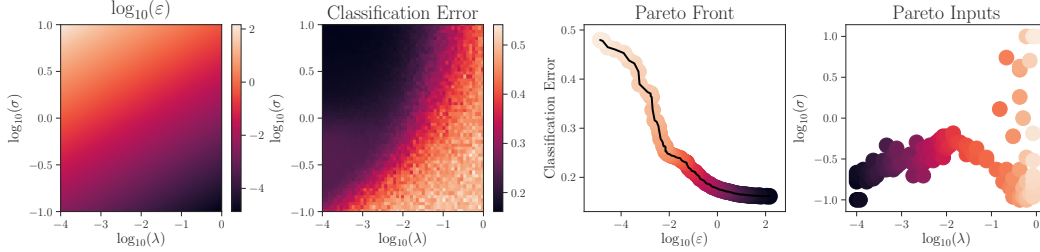


Figure 1: Values returned by the privacy (*far left*) and utility (*center left*) oracles across a range of hyperparameters in the logistic regression example. The Pareto front (*center right*) and set of corresponding input points (marked with stars) (*far right*).

An alternative approach is to assume the existence of a *public* dataset z_0 following a similar distribution to the private dataset z on which we would like to run the algorithm. Then we can use z_0 to compute the Pareto front of the algorithm, select hyperparameters λ^* achieving a desired privacy–utility trade-off, and release the output of $A_{\lambda^*}(z)$. In particular, this the threat model being used by the U.S. Census Bureau to tune the parameters for their use of DP in the context of the 2020 census (see Sec. 5 for more details).

3 DPARETO: Learning the Pareto Front

This section starts by recalling the basic ideas behind multi-objective Bayesian optimization. Then we describe the proposed methodology to learn the privacy–utility Pareto front and revisit the sparse vector technique example to illustrate the effectiveness of our method.

Bayesian Optimization for Multiple Objectives Bayesian optimization (BO) [37] is a strategy for sequential decision making useful for optimizing expensive-to-evaluate black-box objective functions. It has become increasingly relevant in machine learning due to its success in the optimization of model hyperparameters [42, 22].

In its most standard form, BO is used to find the minimum of an objective function $f(\lambda)$ on some subset $\Lambda \subseteq \mathbb{R}^d$ of a Euclidean space of moderate dimension. It works by generating a sequence of evaluations of the objective at locations $\lambda_1, \dots, \lambda_k$, which is done by (i) building a surrogate model of the objective function using the current data and (ii) applying a pre-specified criterion to select a new location λ_{k+1} based on the model. In the single-objective case a common choice is to select the location that, in expectation under the model, gives the best improvement to the current estimate [37].

In this work, we use BO for learning the privacy–utility Pareto front. When used in multi-objective problems, BO aims to learn the Pareto front with a minimal number of evaluations, which makes it an appealing tool in cases where evaluating the objectives is expensive. Although in this paper we only work with two objective functions, we detail here the general case of minimizing p objectives f_1, \dots, f_p simultaneously. This generalization could be used, for instance, to introduce the running time of the algorithm as a third objective to be traded off against privacy and utility.

Let $\lambda_1, \dots, \lambda_k$ be a set of locations in Λ and denote by $\mathcal{V} = \{v_1, \dots, v_k\}$ the set such that each $v_i \in \mathbb{R}^p$ is the vector $(f_1(\lambda_i), \dots, f_p(\lambda_i))$. In a nutshell, BO works by iterating over the following:

1. Fit a surrogate model of the objectives $f_1(\lambda) \dots, f_p(\lambda)$ using the available dataset $\mathcal{D} = \{(\lambda_i, v_i)\}_{i=1}^k$. The most standard approach is to use a Gaussian process (GP) [39].
2. For each objective f_j calculate the predictive distribution over $\lambda \in \Lambda$ using the surrogate model. If GPs are used, the predictive distribution of each output can be fully characterized by their mean $m_j(\lambda)$ and variance $s_j^2(\lambda)$ functions, which can be computed in closed form.
3. Use the posterior distribution of the surrogate model to form an acquisition function $\alpha(\lambda; \mathcal{I})$, where \mathcal{I} represents the dataset \mathcal{D} and the GP posterior conditioned on \mathcal{D} .
4. Collect the next evaluation point λ_{k+1} at the (numerically estimated) global maximum of $\alpha(\lambda; \mathcal{I})$.

The process is repeated until the budget to collect new locations is over. There are two key aspects of any BO method: the surrogate model of the objectives and the acquisition function $\alpha(\lambda; \mathcal{I})$.

In this work we used independent GPs with a transformed output domain to model each objective, but generalizations with multi-output GPs [4] are possible (see Appx. E).

Acquisition with Pareto Front Hypervolume Next we define an acquisition criterion $\alpha(\lambda; \mathcal{I})$ useful to collect new points when learning the Pareto front. Let $\mathcal{P} = \mathcal{PF}(\mathcal{V})$ be the Pareto front computed with the objective evaluations in \mathcal{I} and let $v^\dagger \in \mathbb{R}^p$ be some ‘‘anti-ideal’’ point⁷. To measure the relative merit of different Pareto fronts we use the *hypervolume* $\text{HV}_{v^\dagger}(\mathcal{P})$ of the region dominated by the Pareto front \mathcal{P} bounded by the anti-ideal point. Mathematically this can be expressed as $\text{HV}_{v^\dagger}(\mathcal{P}) = \mu(\{v \in \mathbb{R}^p \mid v \preceq v^\dagger, \exists u \in \mathcal{P} u \preceq v\})$, where μ denotes the standard Lebesgue measure on \mathbb{R}^p . Henceforth we assume the anti-ideal point is fixed and drop it from our notation.

Larger hypervolume means the points in the Pareto front are closer to the ideal point $(0, 0)$. Thus, $\text{HV}(\mathcal{PF}(\mathcal{V}))$ provides a way to measure the quality of the Pareto front obtained from the data in \mathcal{V} . Furthermore, hypervolume can be used to design acquisition functions for selecting hyperparameters that will improve the Pareto front. Start by defining the increment in the hypervolume given a new point $v \in \mathbb{R}^p$: $\Delta_{\mathcal{PF}}(v) = \text{HV}(\mathcal{PF}(\mathcal{V} \cup \{v\})) - \text{HV}(\mathcal{PF}(\mathcal{V}))$. This quantity is positive only if v lies in the set $\tilde{\Gamma}$ of points non-dominated by $\mathcal{PF}(\mathcal{V})$. Therefore, the *probability of improvement* (PoI) over the current Pareto front when selecting a new hyperparameter λ can be computed using the model trained on \mathcal{I} as $\text{Pol}(\lambda) = \mathbb{P}[(f_1(\lambda), \dots, f_p(\lambda)) \in \tilde{\Gamma} \mid \mathcal{I}] = \int_{v \in \tilde{\Gamma}} \prod_{j=1}^p \phi_j(\lambda; v_j) dv_j$, where $\phi_j(\lambda; \cdot)$ is the predictive Gaussian density for f_j with mean $m_j(\lambda)$ and variance $s_j^2(\lambda)$.

The $\text{Pol}(\lambda)$ function accounts for the probability that a given $\lambda \in \Lambda$ has to improve the Pareto front, and it can be used as a criterion to select new points. However, in this work, we opt for the *hypervolume-based PoI* (HVPoI) due to its superior computational and practical properties [11]. The HVPoI is given by $\alpha(\lambda; \mathcal{I}) = \Delta_{\mathcal{PF}}(m(\lambda)) \cdot \text{Pol}(\lambda)$, where $m(\lambda) = (m_1(\lambda), \dots, m_d(\lambda))$. This acquisition weights the probability of improving the Pareto front with a measure of how much improvement is expected computed using the means of the outputs. The HVPoI has been shown to work well in practice and efficient implementations exist.

The DPARETO Algorithm The main optimization loop of DPARETO is shown in Alg. 1. It combines the two ingredients sketched so far: GPs for surrogate modelling of the objective oracles, and HVPoI as an acquisition function to select new hyperparameters. The basic procedure is to first seed the optimization by selecting k_0 hyperparameters from Λ at random, and then fit the GP models for the privacy and utility oracles based on these points. We then find the maximum of the HVPoI acquisition function to obtain the next query point, which is then added into the dataset. This is repeated k times until the optimization budget is used up. Further implementation details are provided in Appx. E.1.

Now we revisit our example on private logistic regression with SGD and output perturbation from Sec. 3 to illustrate how GPs can learn a good model of the privacy and utility oracles from a few random samples and how that produces an acquisition function to find next hyperparameter settings that improve the current empirical Pareto front. This corresponds to the initialization phase of DPARETO; results are given in Figure 2.

4 Experiments

We provide experimental evaluation of DPARETO on a number of ML tasks, highlighting the advantage of using BO over random or grid search, and showcasing DPARETO’s versatility on a variety of models, datasets and optimizers. Due to space limitations, further details (e.g. optimization domains and random sampling distributions) and additional results are given in Appx. C and Appx. D.

Datasets We tackle two classic problems: multiclass classification of handwritten digits with the MNIST dataset, and binary classification of income with the ADULT dataset. MNIST [29] is composed of 28×28 gray-scale images, each representing a single digit 0-9. It has 60k (10k) images in the training (test) set. ADULT [26] is composed of 123 binary demographic features on various people, with the task of predicting whether income $> \$50k$. It has 40k (1.6k) points in the training (test) set.

⁷The anti-ideal point must be dominated by all points in $\mathcal{PF}(\mathcal{V})$. See [11] for further details.

Algorithm 1: DPARETO

Input: $\Lambda, P_\delta, U_z, v^\dagger, k_0, k$

Initialize dataset $\mathcal{D} \leftarrow \emptyset$

for $i \in [k_0]$ **do**

Sample random point $\lambda \in \Lambda$

Evaluate oracles $v \leftarrow (P_\delta(\lambda), 1 - U_z(\lambda))$

Augment dataset $\mathcal{D} \leftarrow \mathcal{D} \cup \{(\lambda, v)\}$

for $i \in [k]$ **do**

Fit GPs to transformed privacy and utility using \mathcal{D}

Obtain new query point λ by optimizing HVPoI using anti-ideal point v^\dagger

Evaluate oracles $v \leftarrow (P_\delta(\lambda), 1 - U_z(\lambda))$

Augment dataset $\mathcal{D} \leftarrow \mathcal{D} \cup \{(\lambda, v)\}$

return Pareto front $\mathcal{PF}(\{v \mid (\lambda, v) \in \mathcal{D}\})$

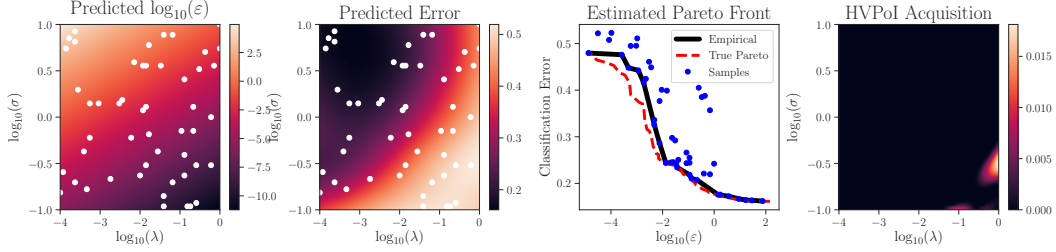


Figure 2: Mean predictions of ε (*far left*) and utility (*center left*) using GP models. In white the locations of the $k_0 = 50$ sampled points are plotted. Empirical and true Pareto fronts (*center right*) and HVPoI function derived from GPs to select the next location.

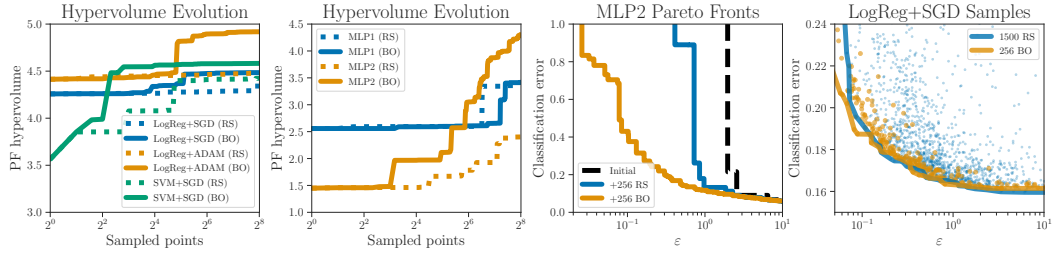


Figure 3: *Far left, center left*: Hypervolumes of the Pareto fronts computed by the various models, optimizers, and architectures on the ADULT and MNIST datasets (respectively) by both DPARETO and random sampling. *Center right*: Pareto fronts learned for MLP2 architecture on the MNIST dataset with DPARETO and random sampling, including the shared points they were both initialized with. *Far right*: ADULT dataset DPARETO sampled points and its Pareto front compared to larger set of random sampling points and its Pareto front.

Algorithms Experiments are performed with privatized variants of two popular optimization algorithms – stochastic gradient descent (SGD) [7] and Adam [23] – although our framework can easily accommodate other algorithms. For the privatized version of SGD, we use a mini-batched implementation with clipped gradients and Gaussian noise similar to that of [1], where the only difference is that we sample mini-batches of a fixed size without replacement instead of sampling mini-batches from a Poisson distribution with fixed rate, and use the moments accountant from [44]. Our privatized version of Adam uses the same gradient perturbation technique as SGD. The pseudo-code for both of these can be found in Appx. B (Alg. 4 and Alg. 5 respectively).

Models For ADULT dataset, we consider logistic regression (LogReg) and linear support vector machines (SVMs), and explore the effect of the choice of model and optimization algorithm (SGD vs. Adam), using the differentially private versions of these algorithms outlined in Appx. B. For MNIST, we fix the optimization algorithm as SGD, but use a more expressive multilayer perceptron (MLP) model and explore the choice of network architectures. The first (MLP1) has a single hidden layer with 1000 neurons, which is the same as used by [1] but without PCA dimensionality reduction. The second (MLP2) has two hidden layers with 128 and 64 units. In both cases we use ReLU activations.

DPARETO vs. Random Sampling A primary purpose of these experiments is to highlight the efficacy of DPARETO at estimating the privacy-utility trade-off of a given algorithm. As discussed in above, the hypervolume is a popular measure for quantifying the quality of a Pareto front. We compare DPARETO to the traditional naïve approach of uniform random sampling by computing the hypervolumes of Pareto fronts generated by each method.

In Fig. 3, the first two plots show, for a variety of models, how the hypervolume of the Pareto front expands as new points are sampled. In nearly every experiment, DPARETO’s approach yields a greater hypervolume than the experiment’s random sampling analog – a direct indicator that DPARETO has better characterized the Pareto front. This can be seen very clearly by examining the center right plot of the figure, which directly shows a Pareto front of the MLP2 model with both sampling methods. Specifically, while the random sampling method only marginally improved over its initially seeded points, DPARETO was able to thoroughly explore the high-privacy regime (i.e. small ε). The far right plot of the figure compares the DPARETO approach with 256 sampled points against the random sampling approach with significantly more sampled points, 1500. While both approaches yield similar Pareto fronts, the efficiency of DPARETO is particularly highlighted by the points that

are not actually on the front: nearly all the points chosen by DPARETO are close to the actual front, whereas many points chosen by random sampling are nowhere near it. We also ran experiments using grid search, where we chose used grid sizes of 3 or 4 (corresponding to 243 and 1024 points), both of which performed clearly worse than DPARETO. These are shown in Fig. 8 in Appx. D.

To quantify the differences between random sampling and DPARETO for the ADULT dataset, we split the 5000 random samples into 19 parts of size 256 to match the number of BO points, and computed hypervolume differences between the resultant Pareto fronts under the (mild) assumption that DPARETO is deterministic⁸. We then computed the two-sided confidence intervals for these differences, shown in Table 1. We also computed the t-statistic for these differences being zero, which were all highly significant ($p < 0.001$). This demonstrates that the observed differences between Pareto fronts are in fact statistically significant. We did not have enough random samples to run statistical tests for MNIST, however the differences are visually even clearer in this case.

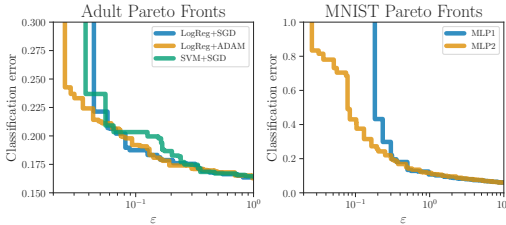


Figure 4: *Left*: Pareto fronts for combinations of models and optimizers on the ADULT dataset. *Right*: Pareto fronts for different MLP architectures on the MNIST dataset.

Algorithm+ Optimizer	Mean difference	95% C.I.
LogReg+SGD	0.158	(0.053, 0.264)*
LogReg+ADAM	0.439	(0.272, 0.607)*
SVM+SGD	0.282	(0.161, 0.402)*

Table 1: Mean hypervolume differences between BO and 19 random repetitions of 256 iterations of random sampling. Two-sided 95% confidence intervals (C.I.) for these differences, as well as t-tests for the mean, are included. Asterisks indicate significance at the $p < 0.001$ level.

DPARETO’s Versatility The other main purpose of these experiments is to demonstrate the versatility of DPARETO by comparing multiple approaches to the same problem. In Fig. 4, the left plot shows Pareto fronts of the ADULT dataset for multiple optimizers (SGD and Adam) as well as multiple models (LogReg and SVM), and the right plot shows Pareto fronts of the MNIST dataset for different architectures (MLP1 and MLP2). With this, we can see that on the ADULT dataset, the LogReg model optimized using Adam was nearly always better than the other model/optimizer combinations. We can also see that on the MNIST dataset, while both architectures performed similarly in the low-privacy regime, the MLP2 architecture significantly outperformed the MLP1 architecture in the high-privacy regime. With DPARETO, analysts and practitioners can efficiently create these types of Pareto fronts and use them to perform privacy–utility trade-off comparisons.

5 Related Work

While this work is the first to examine the privacy–utility trade-off of differentially private algorithms using multi-objective optimization and Pareto fronts, efficiently computing Pareto fronts without regards to privacy is an active area of research in fields relating to multi-objective optimization. DPARETO’s point-selection process most closely aligns with [12], but other approaches (e.g., [46]) may provide promising alternatives for improving DPARETO.

The threat model and outputs of the DPARETO algorithm are closely aligned with the methodology used by the U.S. Census Bureau to choose the privacy parameter ϵ for their deployment of DP to release data from the upcoming 2020 census. In particular, the bureau is combining a graphical approach to represent the privacy–utility trade-off for their application [18] together with economic theory to pick a particular point to balance the trade-off [3]. Their graphical approach works with Pareto fronts identical to the ones computed by our algorithm, which they construct using data from previous censuses [2]. However, they do not attempt to optimize or learn the Pareto front.

Several aspects of this paper are related to recent work in single-objective optimization. For non-private single-objective optimization, there is an abundance of recent work in machine learning on hyperparameter selection, typically using BO [24, 21] or other methods [30] to maximize a model’s

⁸Whilst this is not strictly true, since BO is seeded with a random set of points, running repetitions would have been an extremely costly exercise, and we would expect the results to be nearly identical

utility. Recently, several related questions at the intersection of machine learning and differential privacy have emerged regarding hyperparameter selection and utility maximization.

One such question explicitly asks how to do the hyperparameter-tuning process in a privacy-preserving way. Specifically, [28] and subsequently [40] use BO to find near-optimal hyperparameter settings for a given model while preserving the privacy of the data during the utility evaluation stage. Aside from the single-objective focus of this setting, our setting is significantly different in that we are primarily interested in *training* the models with differential privacy, not in protecting the privacy of the data used to evaluate an already-trained model.

Another question asks how to choose utility-maximizing hyperparameters when privately training models. When privacy is independent of the hyperparameters, this reduces to the non-private hyperparameter optimization task. However, two variants of this question don't have this trivial reduction. The first variant inverts the stated objective: [31] and [19] each study the problem of maximizing privacy given constraints on the final utility. The second variant, closely aligning with the setting in this paper, studies the problem of choosing utility-maximizing, but privacy-dependent, hyperparameters. This is particularly challenging, since the privacy's dependence on the hyperparameters may be non-analytical and computationally expensive to determine. [34, 43] provide approaches to this variant, however the proposed strategies are 1) based on heuristics, 2) only applicable to the differentially private SGD problem, and 3) do not provide a computationally efficient way to find the Pareto optimal points for the privacy-utility trade-off of a given model. [45] provides a practical analysis-backed approach to privately training utility-maximizing models (again, for the case of SGD with a fixed privacy constraint), but hyperparameter optimization is naïve performed using grid-search. By contrast, this paper provides a computationally efficient way to *directly* search for Pareto optimal points for the privacy-utility trade-off of arbitrary hyperparameterized algorithms.

The final related question revolves around the differentially private “selection” or “maximization” problem [9], which asks: how can an item be chosen (from a predefined universe) to maximize a data-dependent function while still protecting the privacy of that data? Here, [32] recently provided a way to choose hyperparameters that approximately maximize the utility of a given differentially private model in a way that protects the privacy of both the training and test data sets. However, this only optimizes utility with fixed privacy – it doesn't address our problem of directly optimizing for the selection of hyperparameters that generate privacy-utility points which fall on the Pareto front.

Recent work on data-driven algorithm configuration has considered the problem of tuning the hyperparameters of combinatorial optimization algorithms while maintaining DP [5]. In this, problem instances are sampled from a distribution, and this sample's privacy is protected. A similar problem of data-driven algorithm selection is considered by [27], where the problem is to choose the best algorithm to accomplish a given task while maintaining the privacy of the data used. For both, only the utility objective is being optimized, assuming a fixed constraint on the privacy.

6 Conclusion

In this paper we introduced DPARETO, a method to empirically characterize the privacy-utility trade-off of differentially private algorithms. We use Bayesian optimization (BO), a state-of-the-art method for hyperparameter optimization, to simultaneously optimize for both privacy and utility, forming a Pareto front. Further, we showed that BO allows us to perform useful visualizations to aid the decision making process. There are several directions for future work. We focused on supervised learning, but the method could also be applied to, e.g. stochastic variational inference on probabilistic models, as long as a utility function (e.g. held-out perplexity) is available. DPARETO currently uses independent GPs, but an interesting extension would be to use multi-output GPs. While we explored the effect of changing the model (logistic regression vs. SVM) and the optimizer (SGD vs. Adam) on the privacy-utility trade-off, it would be interesting to optimize over these choices as well. Finally, it may be of interest to optimize over additional criteria, such as model size or running time.

References

- [1] M. Abadi, A. Chu, I. Goodfellow, H. B. McMahan, I. Mironov, K. Talwar, and L. Zhang. Deep learning with differential privacy. In *Proceedings of the 2016 ACM SIGSAC Conference on Computer and Communications Security*, pages 308–318. ACM, 2016.
- [2] J. M. Abowd. Disclosure avoidance for block level data and protection of confidentiality in public tabulations. Census Scientific Advisory Committee (Fall Meeting), 2018. URL <https://www2.census.gov/cac/sac/meetings/2018-12/abowd-disclosure-avoidance.pdf>.
- [3] J. M. Abowd and I. M. Schmutte. An economic analysis of privacy protection and statistical accuracy as social choices. *American Economic Review*, *Forthcoming*, 2018.
- [4] M. A. Álvarez, L. Rosasco, and N. D. Lawrence. Kernels for vector-valued functions: A review. *Found. Trends Mach. Learn.*, 4(3):195–266, Mar. 2012. ISSN 1935-8237. doi: 10.1561/22000000036. URL <http://dx.doi.org/10.1561/22000000036>.
- [5] M.-F. Balcan, T. Dick, and E. Vitercik. Dispersion for data-driven algorithm design, online learning, and private optimization. In *2018 IEEE 59th Annual Symposium on Foundations of Computer Science (FOCS)*, pages 603–614. IEEE, 2018.
- [6] B. Balle and Y. Wang. Improving the gaussian mechanism for differential privacy: Analytical calibration and optimal denoising. In *Proceedings of the 35th International Conference on Machine Learning, ICML 2018, Stockholmsmässan, Stockholm, Sweden, July 10-15, 2018*, pages 403–412, 2018.
- [7] L. Bottou. Large-scale machine learning with stochastic gradient descent. In *Proceedings of COMPSTAT'2010*, pages 177–186. Springer, 2010.
- [8] N. Carlini, C. Liu, J. Kos, Ú. Erlingsson, and D. Song. The secret sharer: Measuring unintended neural network memorization & extracting secrets. *CoRR*, abs/1802.08232, 2018.
- [9] K. Chaudhuri, D. J. Hsu, and S. Song. The large margin mechanism for differentially private maximization. In *Advances in Neural Information Processing Systems*, pages 1287–1295, 2014.
- [10] T. Chen, M. Li, Y. Li, M. Lin, N. Wang, M. Wang, T. Xiao, B. Xu, C. Zhang, and Z. Zhang. MXNet: A flexible and efficient machine learning library for heterogeneous distributed systems. *arXiv preprint arXiv:1512.01274*, 2015.
- [11] I. Couckuyt, D. Deschrijver, and T. Dhaene. Fast calculation of multiobjective probability of improvement and expected improvement criteria for Pareto optimization. *Journal of Global Optimization*, 60(3):575–594, 2014.
- [12] I. Couckuyt, D. Deschrijver, and T. Dhaene. Fast calculation of multiobjective probability of improvement and expected improvement criteria for pareto optimization. *Journal of Global Optimization*, 60(3):575–594, 2014.
- [13] C. Dwork. Differential privacy. In *Automata, Languages and Programming, 33rd International Colloquium, ICALP 2006, Venice, Italy, July 10-14, 2006, Proceedings, Part II*, pages 1–12, 2006.
- [14] C. Dwork, F. McSherry, K. Nissim, and A. Smith. Calibrating noise to sensitivity in private data analysis. In *Theory of cryptography conference*, pages 265–284. Springer, 2006.
- [15] C. Dwork, M. Naor, O. Reingold, G. N. Rothblum, and S. Vadhan. On the complexity of differentially private data release: efficient algorithms and hardness results. In *Proceedings of the forty-first annual ACM symposium on Theory of computing*, pages 381–390, 2009.
- [16] C. Dwork, A. Roth, et al. The algorithmic foundations of differential privacy. *Foundations and Trends® in Theoretical Computer Science*, 9(3–4):211–407, 2014.
- [17] V. Feldman, I. Mironov, K. Talwar, and A. Thakurta. Privacy amplification by iteration. In *2018 IEEE 59th Annual Symposium on Foundations of Computer Science (FOCS)*, 2018.

- [18] S. L. Garfinkel, J. M. Abowd, and S. Powazek. Issues encountered deploying differential privacy. In *Proceedings of the 2018 Workshop on Privacy in the Electronic Society*, 2018.
- [19] C. Ge, X. He, I. F. Ilyas, and A. Machanavajjhala. Apex: Accuracy-aware differentially private data exploration. 2019.
- [20] J. Geumlek, S. Song, and K. Chaudhuri. Renyi differential privacy mechanisms for posterior sampling. In *Advances in Neural Information Processing Systems*, pages 5289–5298, 2017.
- [21] D. Golovin, B. Solnik, S. Moitra, G. Kochanski, J. Karro, and D. Sculley. Google vizier: A service for black-box optimization. In *Proceedings of the 23rd ACM SIGKDD International Conference on Knowledge Discovery and Data Mining*, pages 1487–1495. ACM, 2017.
- [22] R. Jenatton, C. Archambeau, J. González, and M. Seeger. Bayesian optimization with tree-structured dependencies. In D. Precup and Y. W. Teh, editors, *Proceedings of the 34th International Conference on Machine Learning*, volume 70 of *Proceedings of Machine Learning Research*, pages 1655–1664, International Convention Centre, Sydney, Australia, 06–11 Aug 2017. PMLR.
- [23] D. P. Kingma and J. Ba. Adam: A method for stochastic optimization. In *Proceedings of International Conference on Learning Representations (ICLR)*, 2015.
- [24] A. Klein, S. Falkner, S. Bartels, P. Hennig, and F. Hutter. Fast bayesian optimization of machine learning hyperparameters on large datasets. *arXiv preprint arXiv:1605.07079*, 2016.
- [25] N. Knudde, J. van der Herten, T. Dhaene, and I. Couckuyt. GPflowOpt: A Bayesian Optimization Library using TensorFlow. *arXiv preprint – arXiv:1711.03845*, 2017. URL <https://arxiv.org/abs/1711.03845>.
- [26] R. Kohavi. Scaling up the accuracy of Naive-Bayes classifiers: a decision-tree hybrid. In *KDD*, volume 96, pages 202–207. Citeseer, 1996.
- [27] I. Kotsogiannis, A. Machanavajjhala, M. Hay, and G. Miklau. Pythia: Data dependent differentially private algorithm selection. In *Proceedings of the 2017 ACM International Conference on Management of Data*, pages 1323–1337. ACM, 2017.
- [28] M. Kusner, J. Gardner, R. Garnett, and K. Weinberger. Differentially private bayesian optimization. In *International Conference on Machine Learning*, pages 918–927, 2015.
- [29] Y. LeCun, L. Bottou, Y. Bengio, and P. Haffner. Gradient-based learning applied to document recognition. *Proceedings of the IEEE*, 1998.
- [30] L. Li, K. Jamieson, G. DeSalvo, A. Rostamizadeh, and A. Talwalkar. Hyperband: A novel bandit-based approach to hyperparameter optimization. *arXiv preprint arXiv:1603.06560*, 2016.
- [31] K. Ligett, S. Neel, A. Roth, B. Waggoner, and S. Z. Wu. Accuracy first: Selecting a differential privacy level for accuracy constrained erm. In *Advances in Neural Information Processing Systems*, pages 2566–2576, 2017.
- [32] J. Liu and K. Talwar. Private selection from private candidates. *arXiv preprint arXiv:1811.07971*, 2018.
- [33] M. Lyu, D. Su, and N. Li. Understanding the sparse vector technique for differential privacy. *Proceedings of the VLDB Endowment*, 2017.
- [34] H. B. McMahan and G. Andrew. A general approach to adding differential privacy to iterative training procedures. *CoRR*, abs/1812.06210, 2018.
- [35] H. B. McMahan, D. Ramage, K. Talwar, and L. Zhang. Learning differentially private recurrent language models. In *International Conference on Learning Representations*, 2018. URL <https://openreview.net/forum?id=BJ0hF1Z0b>.
- [36] I. Mironov. Renyi differential privacy. In *Computer Security Foundations Symposium (CSF), 2017 IEEE 30th*, pages 263–275. IEEE, 2017.

- [37] J. Močkus. On Bayesian methods for seeking the extremum. In *Optimization Techniques IFIP Technical Conference*, pages 400–404. Springer, 1975.
- [38] K. Nissim, T. Steinke, A. Wood, M. Altman, A. Bembenek, M. Bun, M. Gaboardi, D. O’Brien, and S. Vadhan. Differential privacy: A primer for a non-technical audience (preliminary version). *Vanderbilt Journal of Entertainment and Technology Law*, Forthcoming, 2018.
- [39] C. E. Rasmussen and C. K. I. Williams. *Gaussian Processes for Machine Learning (Adaptive Computation and Machine Learning)*. The MIT Press, 2005. ISBN 026218253X.
- [40] M. Smith, M. Álvarez, M. Zwiessle, and N. Lawrence. Differentially private regression with Gaussian processes. In *International Conference on Artificial Intelligence and Statistics*, pages 1195–1203, 2018.
- [41] E. Snelson, Z. Ghahramani, and C. E. Rasmussen. Warped Gaussian processes. In *Advances in neural information processing systems*, pages 337–344, 2004.
- [42] J. Snoek, H. Larochelle, and R. P. Adams. Practical Bayesian optimization of machine learning algorithms. In *Advances in neural information processing systems*, pages 2951–2959, 2012.
- [43] K. L. van der Veen. *A Practical Approach to Differential Private Learning*. PhD thesis, Master’s thesis, University of Amsterdam, Amsterdam, The Netherlands, 2018.
- [44] Y. Wang, B. Balle, and S. Kasiviswanathan. Subsampled Rényi differential privacy and analytical moments accountant. In *Proceedings of the 22nd International Conference on Artificial Intelligence and Statistics (AISTATS)*, 2019.
- [45] X. Wu, F. Li, A. Kumar, K. Chaudhuri, S. Jha, and J. Naughton. Bolt-on differential privacy for scalable stochastic gradient descent-based analytics. In *Proceedings of the 2017 ACM International Conference on Management of Data*, pages 1307–1322. ACM, 2017.
- [46] M. Zuluaga, A. Krause, and M. Püschel. ϵ -pal: an active learning approach to the multi-objective optimization problem. *The Journal of Machine Learning Research*, 17(1):3619–3650, 2016.

A Sparse Vector Technique Analysis

The *sparse vector technique* [15] is a mechanism to privately run m queries against a fixed sensitive database and release under DP the indices of those queries which exceed a certain threshold. The naming of the mechanism reflects the fact that it is specifically designed to have good accuracy when only a small number of queries are expected to be above the threshold. The mechanism has found applications in a number of problems, and several variants of the algorithm have been proposed [33].

To illustrate our framework we use a non-interactive version of the mechanism proposed in [33, Alg. 7]. The mechanism is described in Alg. 2, and is tailored to answer m binary queries $q_i : \mathcal{Z}^n \rightarrow \{0, 1\}$ with sensitivity $\Delta = 1$ and a fixed threshold $T = 1/2$. The privacy and utility of the mechanism are controlled by the noise level b and the bound C on the number of answers. Increasing b or decreasing C yields a more private but less accurate mechanism. Unlike in the usual setting, where the sparse vector technique is parametrized by the target privacy ϵ , we modified the mechanism to take as input a total noise level b . This noise level is split across two parameters b_1 and b_2 controlling how much noise is added to the threshold and to the query answers respectively⁹. The standard privacy analysis of the sparse vector technique provides the following closed-form privacy oracle for our algorithm: $P_0 = (1 + (2C)^{1/3})(1 + (2C)^{2/3})b^{-1}$ (see Appx. A for more details).

Algorithm 2: Sparse Vector Technique

Input: dataset z , queries q_1, \dots, q_m
Hyperparameters: noise b , bound C
 $c \leftarrow 0, w \leftarrow (0, \dots, 0) \in \{0, 1\}^m$
 $b_1 \leftarrow b/(1 + (2C)^{1/3}), b_2 \leftarrow b - b_1, \rho \leftarrow \text{Lap}(b_1)$
for $i \in [m]$ **do**
 $v \leftarrow \text{Lap}(b_2)$
 if $q_i(z) + v \geq \frac{1}{2} + \rho$ **then**
 $w_i \leftarrow 1, c \leftarrow c + 1$
 if $c \geq C$ **then return** w
return w

As a utility oracle we use the F_1 -score between the vector of true answers $(q_1(z), \dots, q_m(z))$ and the vector w returned by the algorithm. This measures how well the algorithm identifies the support of the queries that return 1, while penalizing both for false positives and false negatives. This is again different from the usual utility analysis of sparse vector technique algorithms, which focuses on providing an interval around the threshold outside which the output is guaranteed to have no false positives or false negatives [16]. Our measure of utility is more fine-grained and relevant for practical applications, although to the best of our knowledge no theoretical analysis of the utility of the sparse vector technique in terms of F_1 -score is available in the literature.

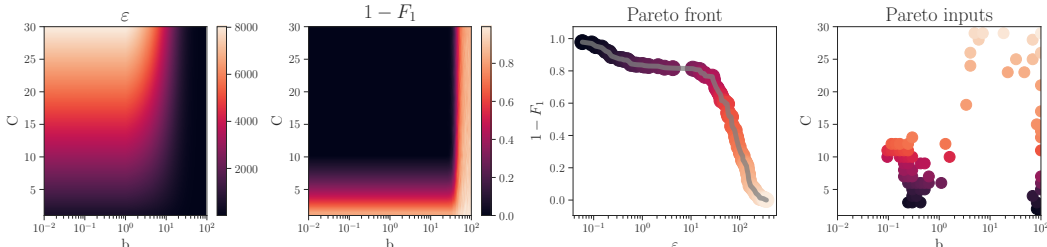


Figure 5: Values returned by the privacy (*far left*) and utility (*center left*) oracles across a range of hyperparameters in the sparse vector technique example. The Pareto front (*center right*) and set of corresponding input points (marked with stars) (*far right*).

To illustrate the concepts introduced in Sec. 2 we compute the oracles and Pareto front for Alg. 2. In our experiment we set $m = 100$ and pick queries at random such that exactly 10 of them return a 1. Since the accuracy of the algorithm is sensitive to the order of the queries, to evaluate the privacy

⁹The split used by the algorithm is based on the privacy budget allocation suggested in [33, Section 4.2].

oracle we run the algorithm 50 times with a random order in the queries and return the average utility. Fig. 5 displays the values returned by the privacy and utility oracles across a range of hyperparameters (left two figures), the Pareto front (center right) and a set of (C, b) pairs that lead to points in the Pareto front (far right).

In this example we were able to compute the Pareto front of Alg. 2 using a simple grid-search procedure on a low-dimensional hyperparameter space. However, this approach might not be computationally feasible in practical applications with more hyperparameters, especially in cases where each evaluation of the utility oracle requires training a machine learning model – thus motivating the DPARETO algorithm.

We now illustrate how DPARETO can help to efficiently learn the privacy–utility trade off. In this example we initialize the GP models with $k_0 = 250$ hyperparameter pairs (C_i, b_i) . The values of C_i are sampled uniformly between 1 and 30. The values of b_i are sampled uniformly in the interval $[0.1, 100]$ on a logarithmic scale. The oracle values for ε and the utility are computed for the selected samples using the same oracles as above. The predicted means of the surrogate models for both oracles are shown in Fig. 6. We observe that both models achieve a reasonably good prediction accuracy when comparing directly to the true values in Fig. 5.

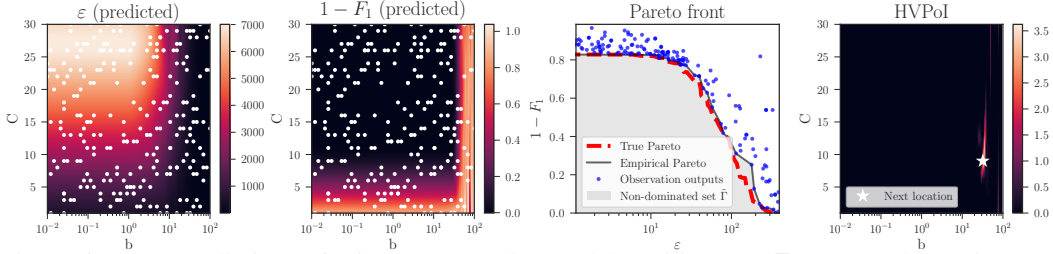


Figure 6: Mean predictions of privacy (ε) (*far left*) and the utility ($1 - F_1$) (*center left*) using two GPs models. In white the locations of the sampled points are plotted. *Center left*: Empirical and true Pareto fronts. *Far right*: HVPoI and the selected next location.

Fig. 6 (center right) shows the exact Pareto front of the problem, along with the output values of the initial sample and the corresponding empirical Pareto front. The empirical Pareto front sits close to the true one, which indicates that the selection of points (C_i, b_i) is already quite good. The goal of DPARETO is to select new points in the input domain whose outputs will bring the empirical front closer to the true one. The HVPoI function $\text{PoI}(\lambda)$ is used for this aim. Fig. 6 (far right) shows the values of the HVPoI for all (C, b) pairs. The maximizer of this function (marked with a star) is used as the next location to evaluate the oracles. Note that given the current models the HVPoI is making a sensible choice, selecting a point where ε is predicted to have a medium value while and $1 - F_1$ is predicted to be low, possibly looking to improve the gap in the lower right corner in the Pareto front plot.

A.1 Privacy Proof

This section provides a proof of the privacy bound for Alg. 2 used to implement the privacy oracle P_0 . The proof is based on observing that our Alg. 2 is just a simple re-parametrization of [33, Alg. 7] where some of the parameters have been fixed up-front. For concreteness, we reproduce [33, Alg. 7] as Alg. 3 below. The result then follows from a direct application of [33, Thm. 4], which shows that Alg. 3 is $(\varepsilon_1 + \varepsilon_2, 0)$ -DP.

Comparing Alg. 3 with the sparse vector technique in Alg. 2, we see that they are virtually the same algorithms, where we have fixed $\Delta = 1$, $T_i = 1/2$, $\varepsilon_1 = 1/b_1$ and $\varepsilon_2 = 2C/b_2$. Thus, by expanding the definitions of b_1 and b_2 as a function of b and C , we can verify that Alg. 2 is $(\varepsilon, 0)$ -DP with

$$\varepsilon = \varepsilon_1 + \varepsilon_2 = \frac{1}{b_1} + \frac{2C}{b_2} = \frac{1 + (2C)^{1/3}}{b} + \frac{(2C)^{2/3}(1 + 2C)^{1/3}}{b} = \frac{(1 + (2C)^{1/3})(1 + (2C)^{2/3})}{b}.$$

This concludes the proof.

Algorithm 3: Sparse Vector Technique ([33, Alg. 7] with $\varepsilon_3 = 0$)

Input: dataset z , queries q_1, \dots, q_m , sensitivity Δ
Hyperparameters: bound C , thresholds T_1, \dots, T_m , privacy parameters $\varepsilon_1, \varepsilon_2$
 $c \leftarrow 0, w \leftarrow (\perp, \dots, \perp) \in \{\perp, \top\}^m$
 $\rho \leftarrow \text{Lap}(\Delta/\varepsilon_1)$
for $i \in [m]$ **do**
 $\nu \leftarrow \text{Lap}(2C\Delta/\varepsilon_2)$
 if $q_i(z) + \nu \geq T_i + \rho$ **then**
 $w_i \leftarrow \top, c \leftarrow c + 1$
 if $c \geq C$ **then return** w
return w

B Differentially Private Stochastic Optimization Algorithms

Stochastic gradient descent (SGD) is a simplification of gradient descent, where on each iteration instead of computing the gradient for the entire dataset, it is instead estimated on the basis of a single example (or small batch of examples) picked uniformly at random (without replacement) [7]. Adam [23] is a first-order gradient-based optimization algorithm for stochastic objective functions, based on adaptive estimates of lower-order moments.

As a privatized version of SGD, we use a mini-batched implementation with clipped gradients and Gaussian noise similar to that of [1]. The pseudo-code is given in Alg. 4; the only difference with the algorithm in [1] is that we sample mini-batches of a fixed size without replacement instead of using mini-batches obtained from Poisson sampling with a fixed probability. In the pseudo-code below, the function $\text{clip}_L(v)$ acts as the identify if $\|v\|_2 \leq L$, and otherwise returns $(L/\|v\|_2)v$. This clipping operation ensures that $\|\text{clip}_L(v)\|_2 \leq L$ so that the ℓ_2 -sensitivity of any gradient to a change in one datapoint in z is always bounded by L/m .

Algorithm 4: Differentially Private SGD

Input: dataset $z = (z_1, \dots, z_n)$
Hyperparameters: learning rate η , mini-batch size m , number of epochs T , noise variance σ^2 , clipping norm L
Initialize $w \leftarrow 0$
for $t \in [T]$ **do**
 for $k \in [n/m]$ **do**
 Sample $S \subset [n]$ with $|S| = m$ uniformly at random
 Let $g \leftarrow \frac{1}{m} \sum_{j \in S} \text{clip}_L(\nabla \ell(z_j, w)) + \frac{2L}{m} \mathcal{N}(0, \sigma^2 I)$
 Update $w \leftarrow w - \eta g$
return w

Our privatized version of Adam is given in Alg. 5, which uses the same gradient perturbation technique as stochastic gradient descent. Here the notation $g^{\odot 2}$ denotes the vector obtained by squaring each coordinate of g . Adam uses three numerical constants that are not present in SGD (κ , β_1 and β_2). To simplify our experiments we fixed those constants to the defaults suggested in [23].

C Experimental Setup

In all our experiments we used $v^\dagger = (10, 1)$ as the anti-ideal point in DPARETO.

C.1 Optimization Domains

Table 2 gives the optimization domain Λ for each of the different experiments.

Algorithm 5: Differentially Private Adam

Input: dataset $z = (z_1, \dots, z_n)$ **Hyperparameters:** learning rate η , mini-batch size m , number of epochs T , noise variance σ^2 , clipping norm L Fix $\kappa \leftarrow 10^{-8}$, $\beta_1 \leftarrow 0.9$, $\beta_2 \leftarrow 0.999$ Initialize $w \leftarrow 0$, $\mu \leftarrow 0$, $\nu \leftarrow 0$, $i \leftarrow 0$ **for** $t \in [T]$ **do** **for** $k \in [n/m]$ **do** Sample $S \subset [n]$ with $|S| = m$ uniformly at random Let $g \leftarrow \frac{1}{m} \sum_{j \in S} \text{clip}_L(\nabla \ell(z_j, w)) + \frac{2L}{m} \mathcal{N}(0, \sigma^2 I)$ Update $\mu \leftarrow \beta_1 \mu + (1 - \beta_1)g$, $\nu \leftarrow \beta_2 \nu + (1 - \beta_2)g^{\odot 2}$, $i \leftarrow i + 1$ De-bias $\hat{\mu} \leftarrow \mu / (1 - \beta_1^i)$, $\hat{\nu} \leftarrow \nu / (1 - \beta_2^i)$ Update $w \leftarrow w - \eta \hat{\mu} / (\sqrt{\hat{\nu}} + \kappa)$ **return** w

Algorithm	Dataset	Epochs (T)	Lot Size (m)	Learning Rate (η)	Noise Variance (σ^2)	Clipping Norm (L)
LogReg+SGD	ADULT	[1, 64]	[8, 512]	[5e-4, 5e-2]	[0.1, 16]	[0.1, 4]
LogReg+Adam	ADULT	[1, 64]	[8, 512]	[5e-4, 5e-2]	[0.1, 16]	[0.1, 4]
SVM+SGD	ADULT	[1, 64]	[8, 512]	[5e-4, 5e-2]	[0.1, 16]	[0.1, 4]
MLP1+SGD	MNIST	[1, 400]	[16, 4000]	[1e-3, 5e-1]	[0.1, 16]	[0.1, 12]
MLP2+SGD	MNIST	[1, 400]	[16, 4000]	[1e-3, 5e-1]	[0.1, 16]	[0.1, 12]

Table 2: Optimization domains used in each of the experimental settings.

C.2 Random Sampling Distributions

The random sampling distributions for experiments with both MNIST and ADULT datasets were chosen to generate as favorable results from the random samplings as possible. The distributions were chosen both from reviewing literature – namely, [1] and [35] – as well as the authors’ experience from training these differentially private models. We note that these distributions generated significantly better points (with regards to characterizing the Pareto front) than naively sampling from the uniform distribution.

Table 3 lists the distributions for the hyperparameters used in the MNIST experiments, and Table 4 lists the distributions for the hyperparameters used in the ADULT experiments.

Hyperparameter	Base Distribution	Parameters	Round-to-Int	Acceptable Range
Epochs	Uniform	$a = 1, b = 400$	True	[1, 400]
Lot Size	Normal	$\mu = 800, \sigma = 800$	True	[16, 4000]
Learning Rate	Shifted Exponential	$\lambda = 10, \text{shift} = 1e-3$	False	[1e-3, 5e-1]
Noise Variance	Shifted Exponential	$\lambda = 5e-1, \text{shift} = 1e-1$	False	[1e-1, 16]
Clipping Norm	Shifted Exponential	$\lambda = 5e-1, \text{shift} = 1e-1$	False	[1e-1, 12]

Table 3: MNIST random sampling distributions.

Hyperparameter	Base Distribution	Parameters	Round-to-Int	Acceptable Range
Epochs	Uniform	$a = 1, b = 64$	True	[1, 64]
Lot Size	Normal	$\mu = 128, \sigma = 64$	True	[8, 512]
Learning Rate	Shifted Exponential	$\lambda = 10, \text{shift} = 1e-3$	False	[1e-3, 1e-1]
Noise Variance	Shifted Exponential	$\lambda = 1e-1, \text{shift} = 1e-1$	False	[1e-1, 16]
Clipping Norm	Shifted Exponential	$\lambda = 1e-1, \text{shift} = 1e-1$	False	[1e-1, 4]

Table 4: ADULT random sampling distributions.

D Further Experimental Results

DPARETO also allows us to gather information about the potential variability of the recovered Pareto front. To that, recall that in our experiments we implemented the utility oracle by repeatedly running algorithm A_λ with a fixed choice of hyperparameters, and then reported the average utility across runs. Using these same runs we can also take the best and worst utilities observed for each choice of hyperparameters. Fig. 7 displays the Pareto fronts recovered from considering the best and worst runs in addition to the Pareto front obtained from the average over runs. In general we observe higher variability in utility on the high privacy regime (i.e. small ϵ), which is to be expected since more privacy is achieved by increasing the variance of the noise added to the computation. These type of plots can be useful to decision-makers who want to get an idea of what variability can be expected in practice from a particular choice of hyperparameters.

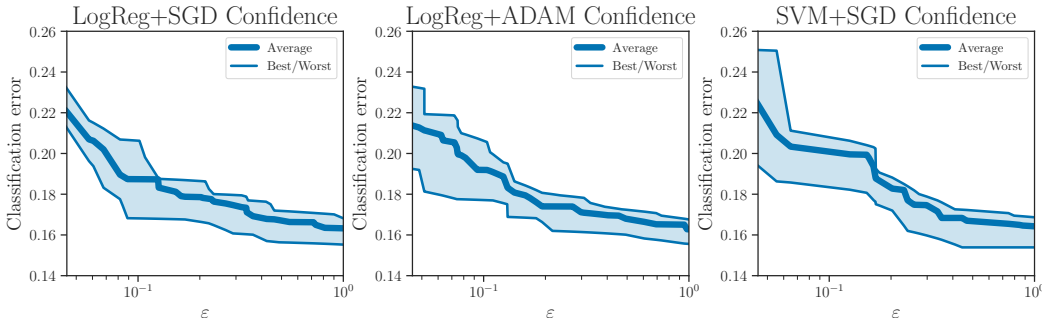


Figure 7: Variability in the Pareto fronts recovered in Sec. 4 on the ADULT dataset.

D.1 Grid Search

For the grid search experiments we have defined parameter ranges as limits of the parameter values from our random sampling experiment setup (see Table 4). We have tried grid size 3, which corresponds to 243 points (approximately the same amount of points as DPARETO uses), and grid size 4, which corresponds to 1024 points (4 times more than what we used for DPARETO). As can be seen in Fig. 8, DPARETO clearly outperformed grid search.

E Implementation Details

E.1 DPARETO

Hyperparameter optimization was implemented with GPFLOW library [25] which offers GP-based Bayesian optimization, as well as the HVPoI acquisition function.

Transformed Output Domains The output domain for accuracy is $[0, 1]$, which would clearly not be modeled well by a GP that models outputs on the entire real line. The output domain for privacy is on the real line, but it is expressed on a logarithmic scale. Hence, in both cases we transform the outputs, so that we are modeling a GP with Gaussian noise in the transformed space. For accuracy, we use a logit transform $\text{logit}(x) = \log(x) - \log(1 - x)$ which transforms values from $[0, 1]$ to $[-\infty, +\infty]$. For privacy, we use a simple log transform. Note that it is possible to use Warped GPs [41], where the transformation is learnt. Concretely this amounts to adding an additional Jacobian term to the likelihood function that takes the transformation into account. The advantage of this approach is that the form of both the covariance matrix and the nonlinear transformation are learnt simultaneously under the same probabilistic framework. However, for simplicity and efficiency we choose to use fixed transformations.

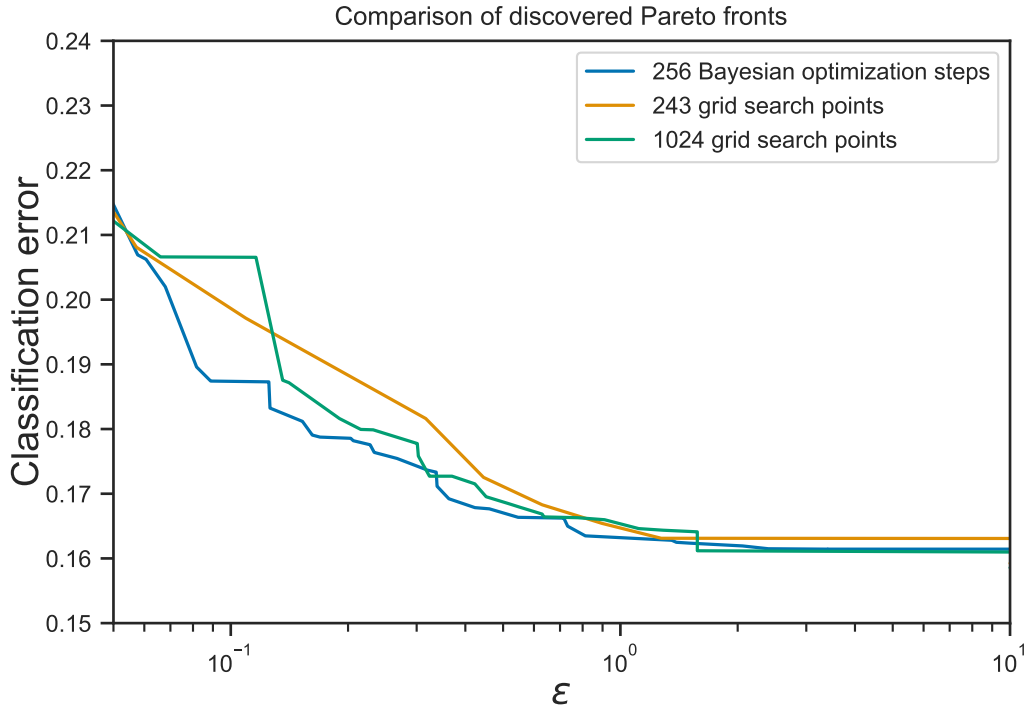


Figure 8: Results of the grid search experiment compared to BO approach used in DPARETO.

E.2 Machine Learning Algorithms and Moments Accountant

Machine learning models used in the paper are implemented with Apache MXNet [10]. We have made use of the high-level Gluon API whenever possible. However, the privacy accountant implementation that we used (see [44]) required low-level changes to the definitions of the models. In order to keep the continuous MXNet execution graph to ensure a fast evaluation of the model, we reverted to the pure MXNet model definitions. Even though this approach requires much more effort to implement the models themselves, it allows for more fine-grained control of how the model is executed, as well as provides a natural way of implementing privacy accounting.